

RESEARCH ARTICLE

A mosquito entomoglyceroporin, *Aedes aegypti* AQP5, participates in water transport across the Malpighian tubules of larvae

Lidiya Misyura, Gil Y. Yerushalmi and Andrew Donini*

ABSTRACT

The mosquito *Aedes aegypti* is the primary vector for arboviral diseases such as Zika fever, dengue fever, chikungunya and yellow fever. The larvae reside in hypo-osmotic freshwater habitats, where they face dilution of their body fluids from osmotic influx of water. The Malpighian tubules help maintain ionic and osmotic homeostasis by removing excess water from the hemolymph; however, the transcellular pathway for this movement remains unresolved. Aquaporins are transmembrane channels thought to permit transcellular transport of water from the hemolymph into the Malpighian tubule lumen. Immunolocalization of *A. aegypti* aquaporin 5 (AaAQP5) revealed expression by Malpighian tubule principal cells of the larvae, with localization to both the apical and basolateral membranes. Knockdown of AaAQP5 with double-stranded RNA decreased larval survival, reduced rates of fluid, K⁺ and Na⁺ secretion by the Malpighian tubules, and reduced Cl⁻ concentrations in the hemolymph. These findings indicate that AaAQP5 participates in transcellular water transport across the Malpighian tubules of larval *A. aegypti* where global AaAQP5 expression is important for larval survival.

KEY WORDS: Mosquito, Water transport, Transcellular, Osmoregulation, Ion-selective microelectrode, Hemolymph

INTRODUCTION

Aedes aegypti (Linnaeus in Hasselquist 1762) mosquitoes inhabit tropical and subtropical climates, where they are vectors for arboviruses such as Zika, chikungunya, dengue and yellow fever (Aitken et al., 1979; Bhatt et al., 2013; Gonzales et al., 2015; Kraemer et al., 2015). The mosquitoes thrive in areas with dense human populations where anthropogenic activities contribute to the accumulation of standing freshwater environments, which are exploited by mosquitoes for the proliferation of larval instars (Kraemer et al., 2015; Rueda, 2008).

The hypo-osmotic freshwater habitats impose an osmotic gradient between the freshwater and larval hemolymph, resulting in the dilution of body fluids, while the concentrated ions passively diffuse out of the body (Bradley, 1987; Marusalin et al., 2012). To overcome this osmotic challenge, osmoregulatory organs including the midgut, Malpighian tubules (MTs), hindgut and the anal papillae work in concert to maintain ionic and osmotic homeostasis.

MTs are composed of principal and stellate cells and are the main osmoregulatory organ removing excess water from the hemolymph, in addition to contributing to xenobiotic detoxification and elimination of nitrogenous waste (Beyenbach and Piermarini, 2011; Esquivel et al., 2016; Wright, 1995). Ions from the hemolymph are transported against their electrochemical gradients into the cytosol of principal and stellate cells, followed by ion secretion into the MT lumen at the apical membrane, a process driven by ion-motive ATPases (Weng et al., 2003). The osmotic drag established by the movement of ions and solutes perpetuates the passive flow of water through the transcellular pathway (Bradley and Snyder, 1989). Studies have indicated a role for aquaporins (AQPs) in water transport through the transcellular pathway in mosquitoes; however, transcellular movement of water has not yet been resolved in mosquito MTs (Drake et al., 2010, 2015; Esquivel et al., 2016; Finn et al., 2015; Overend et al., 2015).

AQPs are integral membrane proteins that are conduits utilized by water and, in some cases, solutes to traverse lipid bilayers (Preston et al., 1993). Six AQP homologues have been identified in the *A. aegypti* genome (*AaAQP1*, *AaAQP2*, *AaAQP3*, *AaAQP4*, *AaAQP5* and *AaAQP6*; nomenclature is that proposed by Drake et al., 2010) (Kambara et al., 2009; Marusalin et al., 2012). AaAQP1 shares the highest sequence homology with the *Drosophila* integral protein (DRIP) family and displays significant water permeability upon its expression in *Xenopus laevis* oocytes (Drake et al., 2015). AaAQP2 is classified as part of the *Pyrocoelia rufa* integral protein (PRIP) family with high water-transport affinity, and a varied tissue expression in adult *A. aegypti* before and after consumption of a blood meal (Campbell et al., 2008; Drake et al., 2015; Marusalin et al., 2012). AaAQP3 is homologous to the *Drosophila* Big Brain (BIB) protein, which has no water-transport capabilities but is rather associated with cell-to-cell adhesion, non-selective cation transport and endosome maturation (Drake et al., 2010; Marusalin et al., 2012). AaAQP6 relative transcript levels have been identified in the adult foregut and the larval anal papillae, but its transport characteristics remain unexplored (Drake et al., 2010; Marusalin et al., 2012).

AaAQP4 and AaAQP5 are members of the entomoglyceroporin (eglp) group of AQPs found only in hexapods, which transport water, urea, glycerol and other polyols (Finn et al., 2015; Van Ekert et al., 2016). Heterologous expression of AaAQP4 confirmed this transporter's glycerol permeability as well as its permeability to urea, erythritol, adonitol, mannitol and trehalose (Drake et al., 2015). However, in this expression system, AaAQP4 was an ineffectual water transporter (Drake et al., 2015). Within the anal papillae of larval *A. aegypti*, AaAQP4 was shown to be salinity responsive, with decreased expression in response to increasing external salinity concentrations (Akhter et al., 2017). In adult mosquitoes, global knockdown of *AaAQP4* resulted in impaired

Department of Biology, York University, 4700 Keele Street, Toronto, ON, Canada M3J 1P3.

*Author for correspondence (adonini@yorku.ca)

 A.D., 0000-0003-2435-2935

Received 16 February 2017; Accepted 26 July 2017

excretion after an injection of phosphate-buffered saline (PBS), which, despite the results of the heterologous expression studies, suggests that AaAQP4 may mediate water transport *in vivo* (Drake et al., 2010). In contrast, AaAQP5 revealed similar water permeability properties as AaAQP1 and was also permeable to trehalose but not to glycerol (Drake et al., 2015). Global knockdown of *AaAQP5* in adult *A. aegypti* injected with PBS resulted in reduced excretion and this, coupled with the results from heterologous expression studies, suggests it plays a role in diuresis and water transport in adults (Drake et al., 2010, 2015). In larvae, AaAQP5 protein expression in anal papillae was elevated under high external salinity (Akhter et al., 2017). These findings suggest that AaAQP5 plays an osmoregulatory role in *A. aegypti*.

In the MTs of larval *A. aegypti* mosquitoes, transcript abundance of *AaAQP1*, *AaAQP4* and *AaAQP5* are highest relative to the other AQPs, leading to the hypothesis that these three AQPs are involved in water transport in these important osmoregulatory organs (Marusalin et al., 2012). In this study, we begin to examine the functional importance of these AQPs in MT function by examining the protein localization and function of AaAQP5 in the MTs of larval mosquitoes. The results begin to elucidate the fundamental molecular basis for water flux across the MT epithelium; one of the most important tissues for the regulation of larval body water levels in freshwater habitats.

MATERIALS AND METHODS

Animal care and survivorship

Aedes aegypti (Liverpool strain) eggs were obtained from a colony reared in the Department of Biology, York University, ON, Canada. Eggs were hatched in 600 ml of reverse-osmosis (RO) water and 6 ml of premade food solution composed of 1.8 g of liver powder and 1.8 g of inactive yeast in 500 ml of RO water. Larvae were kept at room temperature on a 12 h:12 h light:dark cycle for 72 h without additional feeding prior to double-stranded RNA (dsRNA) exposure. Following dsRNA exposure described in detail below, larvae were kept in 20 ml of RO water and fed daily with 1 ml of the food solution described above. Rearing water was refreshed once, 3 days after dsRNA treatment. Survivorship was monitored starting on the second day post-dsRNA treatment through to the sixth day post-dsRNA treatment. Larvae were classified as alive if movement was observed during the counting process.

RNA extraction, dsRNA synthesis and dsRNA exposure

For each sample, 10 larvae were transferred to a tube containing 200 μ l of TRIzol[®] RNA isolation reagent (Invitrogen, Burlington, ON, Canada) and sonicated for 5 s at 5 W using an XL 2000 Ultrasonic Processor (Qsonica LL, Newtown, CT, USA). RNA was extracted according to TRIzol[®] specifications. RNA was treated with the TURBO DNasefree[™] Kit (Applied Biosystems, Mississauga, ON, Canada). The quality and quantity of RNA was determined using a NanoDrop 2000 spectrophotometer (Thermo Scientific, Wilmington, DE, USA). Purified RNA was used to synthesize cDNA with the iScript[™] cDNA Synthesis Kit (Bio-Rad, Mississauga, ON, Canada), according to the manufacturer's instructions. The cDNA was stored at -20°C until subsequent use.

dsRNA synthesis was carried out as previously described by Chasiotis et al. (2016). Using the synthesized cDNA, a fragment of the *AaAQP5* gene (634 bp) with primers (forward 5'-TCATGTACCTTCCACTTCG-3'; reverse 5'-ATTGAGAGCGGTCACTTCA-C-3') designed based on GenBank Accession No. XM_001650119 was amplified using PCR. A fragment of the β -lactamase (β -lac) gene

(799 bp) was also amplified by PCR from a pGEM-T-Easy vector (kind gift from Dr Paluzzi, York University, Toronto, ON, Canada) using the following primers: (forward 5'-ATTTCGTGT-CGCCCTTATTC-3'; reverse 5'-CGTTCATCCATAGTTGCCTG-AC-3'). Using the PCR product as a template, PCR was carried out using the AaAQP5 and β -lac primers with an additional T7 promoter sequence (5'-TAATACGACTCACTATAGGG-3'). PCR products were concentrated and purified using the QIAquick PCR Purification kit (QIAGEN, Toronto, ON, Canada). The purified PCR products were then used as a template to generate dsRNAs by *in vitro* transcription using the Promega T7 RiboMAX Express RNAi Kit (Promega, Fitchburg, WI, USA). Groups of 50–75 larvae (first and second instars), hatched by the method described above, were exposed to 75 μ l of DNase/RNase-free water containing 0.5 $\mu\text{g } \mu\text{l}^{-1}$ of dsRNA for 2 h and later transferred to 20 μ l of RO water. Ingestion of the dsRNA solution by larvae when utilizing this protocol was confirmed previously by Chasiotis et al. (2016).

MT-modified Ramsay secretion assay

Functional experiments were conducted on the MTs of larvae 6 days post-dsRNA treatment. MTs were dissected under physiological saline adapted from Clark and Bradley (1996) and described by Donini et al. (2006) [L-proline 5 mmol l⁻¹, L-glutamine 9.1 mmol l⁻¹, L-histidine 8.74 mmol l⁻¹, L-leucine 14.4 mmol l⁻¹, L-arginine-HCl 3.37 mmol l⁻¹, glucose 10 mmol l⁻¹, succinic acid 5 mmol l⁻¹, malic acid 5 mmol l⁻¹, citric acid (tri-sodium salt) 10 mmol l⁻¹, NaCl 30 mmol l⁻¹, KCl 3 mmol l⁻¹, NaHCO₃ 5 mmol l⁻¹, MgSO₄ 0.6 mmol l⁻¹, CaCl₂ 5 mmol l⁻¹, Hepes 25 mmol l⁻¹] titrated to a final pH of 7.0 using NaOH. Isolated MTs were transferred into 20 μ l droplets of physiological saline contained in wells cut out of a Sylgard[®] (Dow Corning, Mississauga, ON, Canada) lined Petri dish and submerged under paraffin oil. While keeping ~50% of the MT submerged in saline, the proximal end was exposed to the oil and wrapped around a pin adjacent to the saline droplet. The MTs were allowed to secrete fluid for 60 min. Secreted fluid droplets that accumulated at the proximal end of the tubule were then collected for further analysis. The diameter of MT-secreted fluid droplets was measured and the volume of the droplets calculated using the following equation:

$$\text{Volume} = \frac{4}{3} \pi \left(\frac{1}{2} \text{diameter} \right)^3 \quad (1)$$

Fluid secretion rates were calculated by dividing volume by the time it took to secrete the fluid droplets. The Na⁺, K⁺, Ca²⁺ and Cl⁻ concentrations were then measured using the ion-selective microelectrode (ISME) technique described below.

Hemolymph collection and ISME technique

Larvae, 6 days post-dsRNA treatment, were placed on tissue paper to absorb excess external moisture and transferred to a Sylgard[®]-lined Petri dish, filled with paraffin oil (Sigma-Aldrich, Oakville, ON, Canada). A droplet of hemolymph was collected onto the surface of the Sylgard[®] by tearing the cuticle. Concentrations of Na⁺, K⁺, Ca²⁺, Cl⁻ and H⁺ in collected hemolymph droplets were measured using the ISME technique adapted from Jonusaite et al. (2011) and Smith et al. (1999). Liquid membrane ISMEs were constructed using borosilicate glass capillaries (TW150-4; WPI, Sarasota, FL, USA) pulled to a tip diameter of ~5 μ m on a P-97 Flaming Brown micropipette puller (Sutter Instruments Co., Novato, CA, USA) and salinized with vaporized *N,N*-dimethyltrimethylsilylamine at 350 $^{\circ}\text{C}$ for 1 h. The ISMEs were

backfilled with 100 mmol l⁻¹ of appropriate solutions and then front filled with the appropriate ionophore cocktail via capillary action to a column length of 250–300 μm. The backfill solutions and ionophore cocktails (Fluka Analytical, Buchs, Switzerland) used were as follows: Na⁺ (NaCl, Na⁺ Ionophore II Cocktail A); K⁺ (KCl, K⁺ Ionophore I Cocktail B); H⁺ (NaCl, 100 mmol l⁻¹ sodium citrate, pH 6, H⁺ Ionophore I Cocktail B); and Ca²⁺ (CaCl₂, Ca²⁺ Ionophore I Cocktail A). The tips of filled microelectrodes were dipped in a solution of polyvinylchloride (Fluka) in tetrahydrofuran (Fluka) prior to use. The Cl⁻ selective solid-phase microelectrode was constructed as described by Donini and O'Donnell (2005). A reference electrode was constructed by pulling borosilicate glass capillaries (IB200F-4, WPI) on the P97 puller (Sutter Instruments Co.) to a tip diameter of less than 1 μm. The reference microelectrode was filled with 500 mmol l⁻¹ of KCl. The electrodes were connected through an ML 165 pH amplifier to a PowerLab 4/30 data acquisition system (ADInstruments, Colorado Springs, CO, USA) and voltages were recorded and analyzed using LabChart 6 Pro software (ADInstruments). The ISMEs were calibrated after every 4–10 sample readings in the following solutions: Na⁺ (3 mmol l⁻¹ NaCl/297 mmol l⁻¹ LiCl, 30 mmol l⁻¹ NaCl/270 mmol l⁻¹ LiCl and 300 mmol l⁻¹ NaCl); K⁺ (5 mmol l⁻¹ KCl/45 mmol l⁻¹ LiCl and 50 mmol l⁻¹ KCl); Ca²⁺ (0.1 mmol l⁻¹ CaCl₂/299.9 mmol l⁻¹ NaCl, 1 mmol l⁻¹ CaCl₂/299 mmol l⁻¹ NaCl and 10 mmol l⁻¹ CaCl₂/290 mmol l⁻¹ NaCl); H⁺ (200 mmol l⁻¹ NaCl/10 mmol l⁻¹ Hepes, pH 8, 7 and 6); and Cl⁻ (30 mmol l⁻¹ KCl/270 mmol l⁻¹ KHCO₃ and 300 mmol l⁻¹ KCl). The slope measured in mV between the 10-fold concentration differences were within the following range: Na⁺ 54.5–58.5; K⁺ 51–53; Ca²⁺ 24–26; H⁺ 52–56; and Cl⁻ 48–54. Ion concentrations of samples were calculated using the following equation:

$$\text{Ion concentration of sample} = C^a \times 10^{\left(\frac{\Delta V}{m}\right)}, \quad (2)$$

where C^a is the ion concentration of the lower calibration solution, ΔV is the difference in voltage between the sample and the lower calibration solution and m is the slope of the electrode for a 10-fold change in ion concentration.

Immunohistochemistry

Whole guts with intact MTs of *A. aegypti* larvae reared in freshwater were dissected under physiological saline. The guts were transferred to 2% paraformaldehyde in PBS (1.37 mol l⁻¹ NaCl, 0.03 mol l⁻¹ KCl, 0.1 mol l⁻¹ Na₂HPO₄, 0.02 mol l⁻¹ KH₂PO₄; pH 7.4) for 2 h at room temperature (RT) before washing three times for 30 min in PBS at RT. Tissues were blocked with 10% antibody dilution buffer (ADB) [containing 10% goat serum, 3% bovine serum albumin (BSA), 0.05% Triton-X in PBS] at RT for 1 h. Tissues were then incubated for 48 h at 4°C in anti-AaAQP5 affinity purified primary antibody (previously described and validated by Akhter et al., 2017) at a concentration of 2.568 μg μl⁻¹ diluted in ADB or control ADB omitting primary antibody. After incubation, the tissues were washed in PBS three times for 1 h at RT before incubation with the secondary antibody (Alexa Fluor 594-conjugated goat anti-rabbit, dilution 1:500 in ADB) for 24 h in the dark at 4°C. Tissues were washed in PBS three times for 1 h and mounted on slides with ProLong[®] Gold antifade reagent with DAPI (Life Technologies, Burlington, ON, Canada).

Immunohistochemistry of MTs localizing AaAQP5 and V-type H⁺-ATPase was conducted according to a previously published protocol (Chasiotis et al., 2016). Whole larvae were fixed in Bouin's

fixative. Tissues were dehydrated and embedded in paraffin wax. Samples were sectioned on a microtome and placed onto slides for subsequent rehydration and antibody probing. Rabbit anti-AaAQP5 (2.568 μg μl⁻¹ dilution in ADB) and/or guinea pig anti-V-type H⁺-ATPase (kind gift from Dr Weiczorek, University of Osnabruck, Germany, 1:1000 dilution in ADB) antibodies were used to probe the rehydrated tissue samples. A goat anti-rabbit antibody conjugated to AlexaFluor 594 (Jackson ImmunoResearch, West Grove, PA, USA) was applied at 1:500 dilution to visualize AaAQP5, and goat anti-guinea pig antibody conjugated to AlexaFluor 647 (Jackson ImmunoResearch) was applied at 1:500 dilution to visualize V-type H⁺-ATPase. Negative control slides were also processed as described above with all primary antibodies omitted. Slides were mounted using ProLong[®] Gold antifade reagent with DAPI (Life Technologies).

Stained tissues were viewed and images were captured using an Olympus IX81 inverted fluorescent microscope (Olympus Canada, Richmond Hill, ON, Canada) and CellSense[®] 1.12 Digital Imaging software (Olympus Canada). Images were merged using ImageJ 1.49 software (Schneider et al., 2012).

Protein processing, electrophoresis and western blotting

MTs were isolated under physiological saline from 60–75 larvae for each sample 6 days after dsRNA exposure and stored at -80°C until processing. MT samples were sonicated 2×10 s at 3.5 W using an XL 2000 Ultrasonic Processor (Qsonica) in TRIS-HCl homogenization buffer (50 mmol l⁻¹ Tris-HCl, pH 7.4 and 1:200 protease inhibitor cocktail; Sigma-Aldrich). Homogenates were then centrifuged at 16,200 g for 15 min at 4°C using the Sorvall[™] Legend[™] Micro 21 Centrifuge (Thermo Scientific). The protein concentration of the supernatant was measured using DC protein assay (Bio-Rad), according to the manufacturer's guidelines with BSA as a standard. Measurements were carried out on a Multiskan spectrum spectrophotometer (Thermo Scientific) at 750 nm.

Samples were prepared for sodium dodecyl sulphate-polyacrylamide gel electrophoresis (SDS-PAGE) by heating for 5 min at 100°C with 5× loading buffer [225 mmol l⁻¹ Tris-HCl, pH 6.8, 3.5% (w/v) SDS, 35% glycerol, 12.5% (v/v) β-mercaptoethanol and 0.01% (w/v) Bromophenol Blue]. Ten micrograms of protein was loaded onto a 4% stacking and 12% resolving SDS-PAGE gel. Electrophoresis was carried out at 110 V. Proteins were transferred onto a polyvinylidene difluoride (PVDF) membrane using a wet transfer method. Proteins were transferred from the gel at 100 V for 1 h in a cold (~4°C) transfer buffer (0.225 g Tris, 1.05 g glycine in 20% methanol). The PVDF membrane was washed in Tris-buffered saline (TBS-T; 9.9 mmol l⁻¹ Tris, 0.15 mol l⁻¹ NaCl, 0.1 mol l⁻¹ Tween-20, 0.1 mol l⁻¹ NP-40, pH 7.4) for 15 min. The PVDF membrane was then blocked with 5% skimmed milk powder in TBS-T for 1 h at RT and incubated overnight at 4°C with anti-AaAQP5 antibody (1.712 μg μl⁻¹ in 5% skimmed milk in TBS-T). The membrane was then washed four times for 15 min with TBS-T and incubated with horseradish peroxidase (HRP)-conjugated goat anti-rabbit antibody (1:5000 in 5% skimmed milk in TBS-T) (Bio-Rad) for 1 h at RT. PVDF membrane was washed four times for 30 min with TBS-T before carrying out a chemiluminescent reaction using Clarity[™] Western ECL substrate (Bio-Rad). After visualization of detected protein bands, antibodies were washed off of the PVDF membrane using stripping buffer (20 mmol l⁻¹ magnesium acetate, 20 mmol l⁻¹ KCl, 0.1 mol l⁻¹ glycine; pH 2.2) and blocked as described above. Membranes were probed with the anti-β-actin primary antibody (1:1000 in 5% skimmed milk in TBS-T) (Cell

Signalling, Danvers, MA, USA) and HRP-conjugated goat anti-mouse secondary antibody (1:5000 in 5% skimmed milk in TBS-T) (Bio-Rad) as a loading control. ImageJ 1.49 software (Schneider et al., 2012) was used to quantify the protein abundance. The background density of the blot was subtracted from the density of the protein signal. All treatment group densitometry ratios were normalized to a β -actin loading control.

Body moisture measurements

Larvae were placed on tissue paper that absorbed any moisture from the exterior surface of the insect. Larvae were subsequently weighed to the nearest microgram on a UMX2 Automated-S microbalance (Mettler Toledo, Greifensee, Switzerland), dehydrated in a conventional oven at 60°C for 2 days, and reweighed. The mass differential before and after dehydration served as an approximate measure of the total body water content. Values were expressed as a percentage of the total wet body mass.

Statistical analysis

Data were analyzed using GraphPad Prism® 5.03 (GraphPad Software Inc., La Jolla, CA, USA) and expressed as means \pm s.e.m.

Values determined to be significant outliers by the Grubbs' test ($P < 0.05$) were removed from the dataset. All experimental measurements were analyzed using the Student's *t*-test ($P < 0.05$) with the exception of survivorship data where the log-rank (Mantel–Cox) test was used to determine significance ($P < 0.05$).

RESULTS

AaAQP5 immunolocalization in MTs

A custom antibody generated against the C-terminus of *A. aegypti* AaAQP5, validated in Akhter et al. (2017), was used to localize AaAQP5 in the MTs of larval *A. aegypti*. AaAQP5 immunoreactivity was apparent in principal cells where in whole mounts it appeared concentrated at the basal surfaces of the MTs as distinct punctate staining in cytoplasmic or membrane-bound areas (Fig. 1A). Stellate cells, identified by their relatively small nuclei (blue DAPI labeling) and by their intercalating pattern between principal cells, were devoid of any AaAQP5 staining (Fig. 1A, arrows). Cross-sectional images of the MT revealed AaAQP5 staining on both the apical (Fig. 1B, solid arrow) and basal (Fig. 1B, dashed arrow) sides of the epithelial membrane. To further demonstrate the apical localization of AaAQP5 (red,

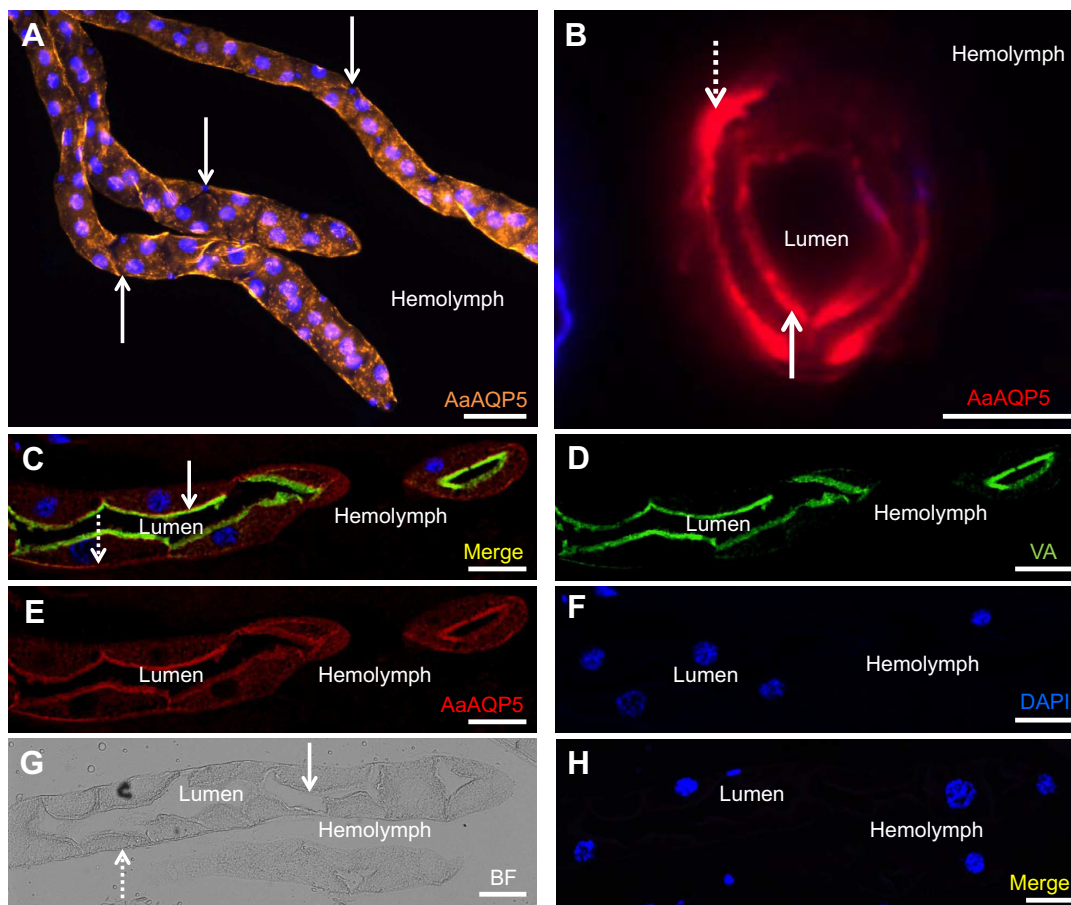


Fig. 1. Immunolocalization of AaAQP5 in the Malpighian tubules (MTs) of larval *Aedes aegypti*. (A) Representative whole-mount MTs illustrating AaAQP5 immunoreactivity in principal cells (orange). Arrows point to stellate cells where AaAQP5 immunoreactivity is absent. Blue staining indicates nuclei labeled with DAPI. (B) Representative paraffin-embedded cross-section of larval MTs showing AaAQP5 immunoreactivity (red staining) on basal (dashed arrow) and apical (solid arrow) sides of principal cells. (C) Representative paraffin-embedded transverse and cross-sections of larval MTs showing AaAQP5 immunoreactivity on the basal side (red, dashed arrow) and AaAQP5 immunoreactivity co-localized with the V_1 subunit of V-type H^+ -ATPase in the apical brush border of principal cells (yellow, solid arrow). Blue staining indicates nuclei labeled with DAPI. (D) Transverse and cross-sections of larval MTs showing immunoreactivity of V_1 subunit of V-type H^+ -ATPase (VA, green) from C. (E) Transverse and cross-sections of larval MTs showing AaAQP5 immunoreactivity (red) from C. (F) Transverse and cross-sections of larval MTs showing DAPI staining (blue) from C. (G) Transverse sections of a control MT in brightfield (BF) demonstrating the apical (solid arrow) and basolateral membranes (dashed arrow). (H) Control transverse sections of MTs from G demonstrating a merge of the control (primary antibodies omitted) and DAPI. Scale bars: (A) 100 μ m; (B–H) 20 μ m.

Fig. 1E), transverse and cross-sectional images of MTs were co-labeled with the apical membrane marker V-type H⁺-ATPase (green, Fig. 1D) and nuclear DAPI (blue, Fig. 1F). In these preparations, AaAQP5 staining was co-localized with V-type H⁺-ATPase staining (Fig. 1C, yellow, solid arrow) on the apical surfaces of principal cells and could also be seen on the basal surfaces (Fig. 1C, red, dashed arrow). We could not co-localize AaAQP5 with a basal marker as we did not have an antiserum for a basal membrane marker of the MTs. Control MTs where the AaAQP5 antisera was omitted from the protocol were devoid of any immunoreactivity (Fig. 1G,H).

Western blotting for AaAQP5 in MTs and AaAQP5 dsRNA treatment

Western blots of MT protein homogenates probed with AaAQP5 antiserum displayed three bands of ~19, 32 and 80 kDa (Fig. 2A). The representative blot demonstrates the three bands; however, not all bands were present in all samples that were probed with the AaAQP5 antisera. While the ~32 kDa band was detected in all blots, the ~19 kDa and ~80 kDa bands were not always detectable. The predicted molecular mass of an AaAQP5 monomer is ~26 kDa. Treatment of larvae with dsRNA targeting AaAQP5 resulted in apparent decreases in the intensity of all three bands detected by the AaAQP5 antiserum in the MT homogenates, relative to those from control larvae treated with dsRNA targeting the bacterial gene β -lac (Fig. 2A). Densitometric analysis was performed on the putative monomer signals (~32 kDa band), which resulted in significantly decreased (48%) putative AaAQP5 monomer protein abundance in the MTs of larvae treated with dsRNA for AaAQP5 relative to those of larvae treated with β -lac dsRNA (unpaired *t*-test, *P*=0.03; Fig. 2B). The putative monomer was not observed when the anti-

AaAQP5 antibody was incubated with the immunogenic peptide (Fig. 2C). The ~80 kDa band could not be evaluated for specificity because the immunogenic peptide bound to higher molecular mass proteins in MT homogenates creating a protein–peptide–antibody interaction.

MT fluid secretion rates, ion concentration of secreted fluid and ion transport rates in dsRNA-treated larvae

MT fluid secretion rates, ion concentration of secreted fluid and ion transport rates of MTs were affected by the knockdown of AaAQP5 (Fig. 3). The transepithelial fluid secretion rate of MTs isolated from larvae treated with dsRNA for β -lac (control) was 0.25 ± 0.02 nl min⁻¹ in comparison with the secretion rate of MTs from AaAQP5 dsRNA-treated larvae, which was significantly lower at 0.17 ± 0.02 nl min⁻¹ (unpaired *t*-test, *P*=0.01). Secreted fluid from the MTs of AaAQP5 dsRNA-treated larvae contained 26% less K⁺ (unpaired *t*-test, *P*=0.004) and 14% less Na⁺ (unpaired *t*-test, *P*=0.01) compared with controls (Fig. 3B). The Cl⁻ concentration of secreted fluid was unaffected by AaAQP5 knockdown and, while Ca²⁺ concentrations appeared lower in AaAQP5 dsRNA treatments, this was not statistically different from controls (unpaired *t*-test, *P*=0.28; Fig. 3B). The product of lower secretion rates and lower K⁺ and Na⁺ concentrations in the secreted fluid resulted in lower K⁺ (unpaired *t*-test, *P*=0.002) and Na⁺ (unpaired *t*-test, *P*=0.002) transepithelial transport rates in the MTs of larvae treated with AaAQP5 dsRNA (Fig. 3C). The K⁺ and Na⁺ transport rates were 50% lower with the AaAQP5 dsRNA treatments. The Ca²⁺ and Cl⁻ transport rates were unaffected by AaAQP5 dsRNA treatment.

Survival, body moisture and hemolymph ion concentration of dsRNA-treated larvae

Survival was measured throughout a 6 day period following larval exposure to dsRNA targeting AaAQP5 or bacterial β -lac (control). Larval survival decreased by 9% (Mantel–Cox test, *P*=0.0011) in larvae treated with AaAQP5 dsRNA relative to larvae treated with β -lac dsRNA (Fig. 4). The greatest number of deaths occurred 3 days following AaAQP5 dsRNA treatment in comparison with β -lac dsRNA treatment. Total body moisture measured 6 days post-dsRNA treatment was similar in larvae treated with AaAQP5 dsRNA and those treated with β -lac dsRNA (unpaired *t*-test, *P*=0.30; Fig. 5). There was also no difference in the hemolymph [K⁺], [Na⁺], [Ca²⁺] and pH between control and AaAQP5 dsRNA-treated larvae; however, the hemolymph [Cl⁻] of AaAQP5 dsRNA-treated larvae was 20% lower than that of control larvae (unpaired *t*-test, *P*=0.003; Fig. 6).

DISCUSSION

Overview

The MTs of *A. aegypti* produce fluid that is iso-osmotic to the hemolymph by actively transporting ions into their lumen, which is followed by osmotic transepithelial transport of water. In freshwater larval mosquitoes, this process is vital to the elimination of excess water, which is continuously accumulating in the hemolymph from the hypo-osmotic habitat (Stobbert, 1971; Wigglesworth, 1932). While the molecular mechanisms for ion transport in the MTs have been studied, those for water movement have received little attention. Currently, it is generally assumed that water crosses the MT epithelium transcellularly through AQPs expressed by the epithelial cells. To date, however, no AQPs have been localized in larval *A. aegypti* MTs, although the transcript abundance of *AaAQP1*, *AaAQP4* and *AaAQP5* are significantly greater than those

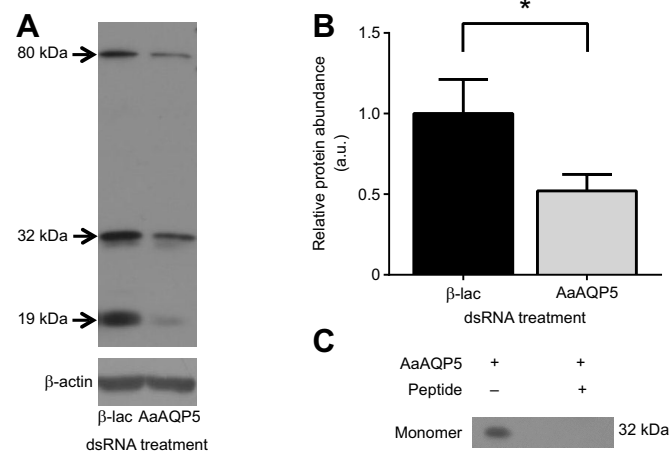


Fig. 2. Western blot of Malpighian tubule (MT) protein homogenates probed with AaAQP5 antisera and effects of double-stranded RNA (dsRNA) treatment on AaAQP5 protein abundance in MTs. (A) Western blot of MT protein homogenates from larvae treated with dsRNA for β -lac (control) or AaAQP5 with β -actin as a loading control. (B) Relative protein abundance of AaAQP5 based on densitometric analysis of putative AaAQP5 monomer (32 kDa) in MT protein homogenates from larvae treated with dsRNA for β -lac or AaAQP5 (*N*=5). The abundance of putative AaAQP5 protein was normalized to β -actin and expressed relative to the control β -lac group. Data are expressed as means \pm s.e.m. *Significant difference from control β -lac group (*P*<0.05, unpaired *t*-test). (C) The putative monomer was blocked by pre-absorption of AaAQP5 antibody with immunogenic peptide. The 19 kDa band did not always appear in blots and assessment of specificity of the 80 kDa band was hindered by the binding of the immunogenic peptide to proteins with higher than ~40 kDa mass.

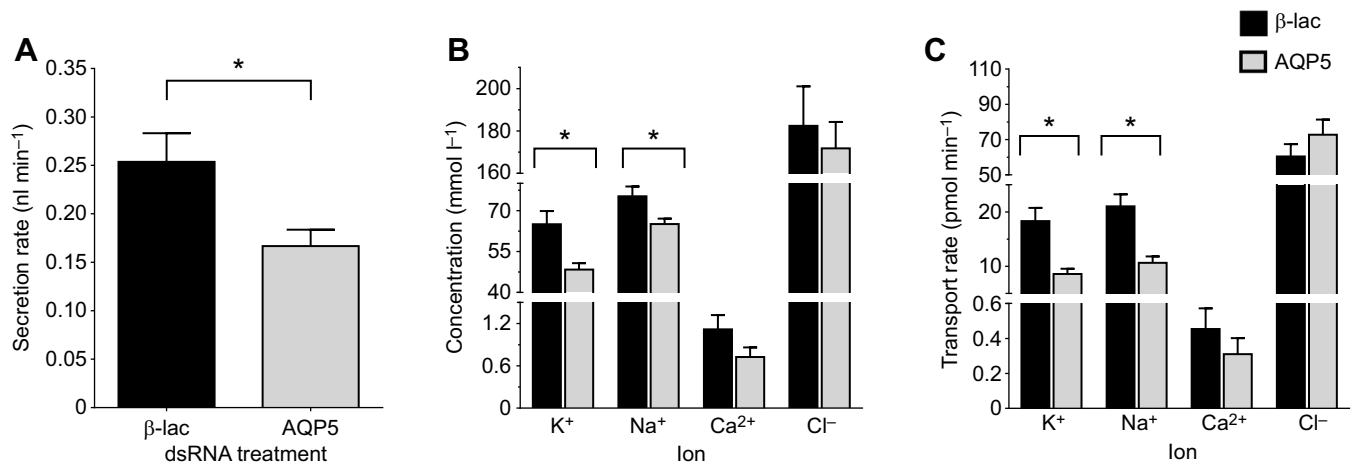


Fig. 3. *In vitro* transepithelial fluid transport rate, ion concentrations in secreted fluid and ion transport rates of Malpighian tubules from larvae treated with double-stranded RNA (dsRNA) targeting β -lac (control) or AaAQP5. (A) Transepithelial fluid transport rate ($N=36$ β -lac and $N=44$ AaAQP5). (B) Ion concentrations of secreted fluid ($N=10$ – 30). (C) Transepithelial ion transport rates calculated as the product of fluid transport rate and ion concentration of secreted fluid ($N=10$ – 44). Data in A–C are expressed as means \pm s.e.m. *Significant difference ($P < 0.05$, unpaired t -test) from control β -lac group.

of the other AQPs (Marusalin et al., 2012). Here, we localized the *A. aegypti* AQP, AaAQP5, to the principal cells of larval MTs and demonstrated that knockdown of AaAQP5 protein expression in the MTs resulted in impaired fluid secretion rates by isolated MTs. These findings indicate that AaAQP5 plays a significant role in transcellular water transport across larval MTs. The knockdown of AaAQP5 in MTs also revealed some unexpected alterations in the ion concentrations of secreted fluid from MTs and ion transport rates of MTs, perhaps suggesting a level of coordination between ion and water transport by MTs.

Expression and localization of AaAQP5 in the MTs

Western blots of larval MT homogenates probed with AaAQP5 antiserum revealed three bands with mass of ~19, 32 and 80 kDa (Fig. 2A). As the predicted mass of an AaAQP5 monomer is 26 kDa, it is suggested that the 19 kDa band represents degradation product arising from protein extraction and subsequent processing. A protein band of 26 kDa immunoreactive to the AaAQP5 antiserum was previously resolved in western blots of larval *A. aegypti* anal papillae homogenates (Akhter et al., 2017). Although AQPs are known to undergo post-translational modifications, this result suggests that a proportion of AaAQP5 monomers in the anal papillae are present without modification (Hendriks et al., 2004; Akhter et al., 2017). In contrast, it is proposed that the AaAQP5 monomers expressed in the MTs undergo modification resulting in the observed 32 kDa band in this study (Fig. 2A). The additional mass of the putative AaAQP5 monomers in the MTs may be attributed to post-translational modification (Hendriks et al., 2004). One such modification may include glycosylation as several invertebrate AQPs have been previously shown to possess glycosylation sites, including AQPs in *Rhodnius prolixus*, *Caenorhabditis elegans* and *A. aegypti* (Echevarría et al., 2001; Pietrantonio et al., 2000; Tomkowiak and Pienkowska, 2010). Alternatively, AQPs can also be phosphorylated to regulate their activity in addition to signaling their translocation into the membrane (Campbell et al., 2008). The variation in the western blot pattern between the anal papillae and the MTs may indicate that post-translational modifications of AQPs may be tissue-specific and may vary to alternatively regulate AaAQP5 function based on its roles in these different tissues. The AaAQP5 immunoreactive 80 kDa band is proposed to represent an

undissociated oligomer. AQP oligomers have been shown to resist dissociation in SDS-PAGE (Cymer and Schneider, 2010; Neely et al., 1999; Smith and Agre, 1991). These oligomers may be homo-oligomers of AaAQP5 with additional post-translational modifications or may be hetero-oligomers of AaAQP5 monomers with monomers of other AQPs (Akhter et al., 2017; Neely et al., 1999).

AaAQP5 expression was localized to the apical and basal membranes of principal cells in larval *A. aegypti* MTs (Fig. 1). Principal cell-specific expression of AQPs has been demonstrated in *Drosophila melanogaster*, where the transcripts of the AaAQP5 functional orthologues, Aqp4019 and Aqp17664, were detected in principal cells using *in situ* hybridization (Kaufmann et al., 2005). In the adult *Anopheles gambiae* mosquito, AgAQP1 protein was localized to stellate cells in the distal portion of the MTs and to principal cells at the proximal end (Liu et al., 2011; Tsujimoto et al., 2013), whereas the DRIP water channel of *D. melanogaster* is restricted to stellate cells of both the larval and adult life stages (Kaufmann et al., 2005). These results demonstrate variability in cell-specific expression between species as well as AQPs. In addition, the punctate AaAQP5 staining in the principal cells of larval *A. aegypti* shown in this study may suggest vesicular localization within the cell (Fig. 1). Intracellular vesicular localization of AQP8 was identified in rat hepatocytes with comparable punctate staining in the cytoplasmic region of the cells (García et al., 2001). Treatment of rat hepatocytes with cAMP resulted in the translocation of vesicular AQP8 into the plasma membrane, which increased membrane water permeability (García et al., 2001). Additionally, in *R. prolixus*, cAMP elevates Rh-MIP (AQP-related protein) expression in the MTs (Martini et al., 2004). The punctate staining of AaAQP5 in larval mosquito MTs may be indicative of a mechanism that is similar to that of AQP8 where modulation of epithelial cell membrane water permeability is facilitated by translocation of intracellularly stored AaAQP5 to the membrane in principal cells. An alternative explanation for the observed punctate staining is the accumulation of AaAQP5 channels at the basolateral or apical membranes. The irregular intensity of immunoreactivity throughout the membranes on the MT cross-section (Fig. 1B) supports the aggregation of AQPs to specific sites on the membrane. Aggregations of AaAQP5 would enable internalization for intracellular storage or degradation in order to

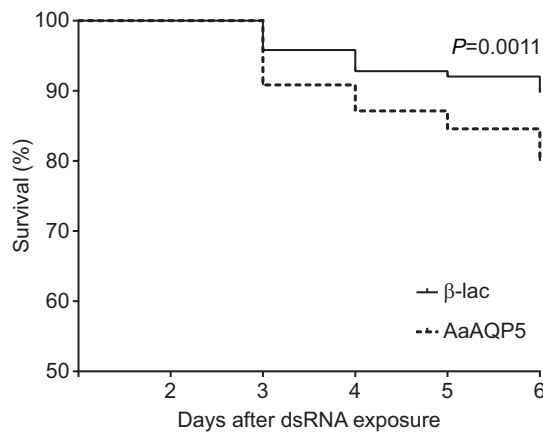


Fig. 4. Larval survival following treatment with β -lac ($N=360$) or AaAQP5 ($N=346$) double-stranded RNA (dsRNA). Data were analyzed using a Mantel–Cox test.

better regulate membrane water permeability. Cell surface punctate immunoreactivity was previously shown for mammalian AQP1 in endothelial cells where it was co-localized with receptors that signal intracellular trafficking and internalization into intracellular vesicles (Kobayashi et al., 2006).

Effects of dsRNA knockdown of AaAQP5 on the MTs of larval *A. aegypti*

Densitometry analysis of the putative AaAQP5 in western blots of MT protein homogenates from the dsRNA β -lac and AaAQP5 treatments demonstrated that phenotypic expression of AaAQP5 was suppressed by 48% (Fig. 2B). The reduced AaAQP5 expression in the MTs of larvae resulted in decreased rates of transepithelial fluid transport (Fig. 3A). A previous study demonstrated increased water and trehalose permeability of *Xenopus* oocytes expressing AaAQP5 (Drake et al., 2015). Taken together, this suggests that the decreased rates of fluid transport are a product of decreased water transport through AaAQP5 resulting from its reduced expression. In addition, the reduced fluid transported across the MT epithelium

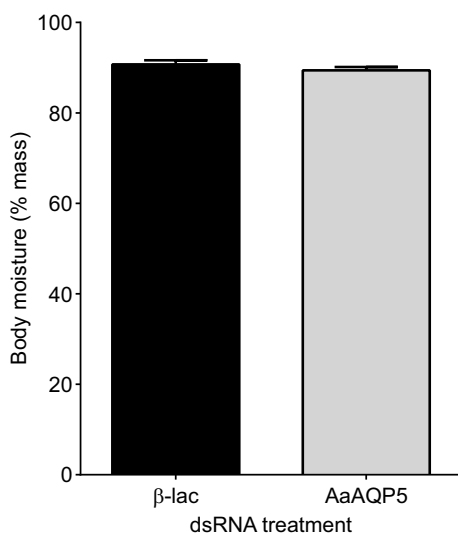


Fig. 5. *Aedes aegypti* total body moisture measured 6 days post-double stranded RNA (dsRNA) treatment for β -lac ($N=18$) and AaAQP5 ($N=13$). Data are expressed as means \pm s.e.m. ($P < 0.05$, ANOVA with Tukey's multiple comparison test).

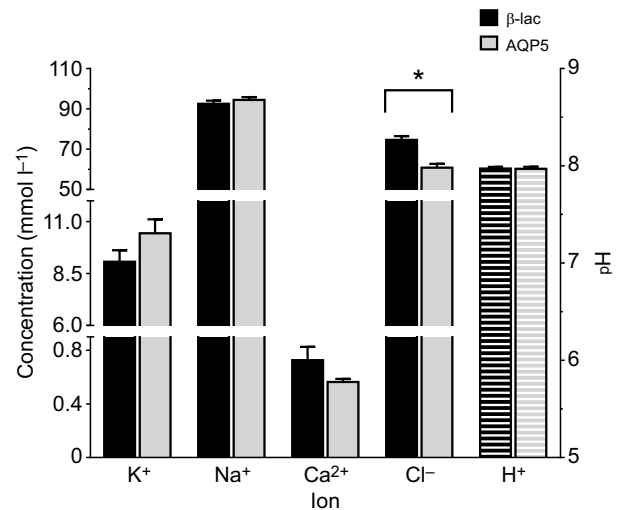


Fig. 6. Hemolymph Na^+ (β -lac $N=23$, AaAQP5 $N=23$), K^+ (β -lac $N=23$, AaAQP5 $N=23$), Ca^{2+} (β -lac $N=30$, AaAQP5 $N=25$), Cl^- (β -lac $N=30$, AaAQP5 $N=25$) concentrations and pH (striped bars) (β -lac $N=10$, AaAQP5 $N=10$) of dsRNA-treated larvae at 6 days post-dsRNA treatment. Data are expressed as means \pm s.e.m. *Significant difference ($P < 0.05$, unpaired t -test) from control β -lac group.

may further be suppressed as a result of reduced osmotic drag established by trehalose transport through AaAQP5 (Drake et al., 2015). Global knockdowns of several AQPs, including AaAQP5 in the adult female *A. aegypti*, resulted in diminished urine excretion following PBS injections (Drake et al., 2010). Furthermore, combined RNAi-mediated knockdown of two AQPs, *gmmDrip* and *gmmDripb*, in the tsetse fly similarly attenuated diuresis by up to 50% (Benoit et al., 2014). The reduction in volume of urine excreted may, in part, be influenced by compromised water transport across the MTs in the adult mosquitoes and the tsetse flies, similar to the findings observed with the larval MTs in this study (Drake et al., 2010; Hegarty et al., 1992; Petzel et al., 1999; Williams and Beyenbach, 1983). Suppression of water transport rates of MTs with diminished AaAQP5 expression in conjunction with the localization of AaAQP5 to the basolateral and apical membranes indicates that AaAQP5 participates in transcellular transport of water across the MT epithelium in larval mosquitoes but does not preclude the involvement of other AQPs that remain to be studied, in particular AaAQP1 and AaAQP4, which show high levels of transcript abundance in the MTs.

The composition of the MT secretion fluid collected in AaAQP5 knockdown larvae had diminished $[Na^+]$ and $[K^+]$, whereas $[Ca^{2+}]$ and $[Cl^-]$ remained unaffected (Fig. 3B). If basal ion transport rates of Na^+ and K^+ across the principal cells remained unaltered while AaAQP5 expression and water transport were reduced, it would be reasonable to expect dilution of the hemolymph. This was not the case as both Na^+ and K^+ transport rates of MTs were reduced and hemolymph $[Na^+]$ and $[K^+]$ were unaffected by AaAQP5 knockdown. Therefore, the reduced $[Na^+]$ and $[K^+]$ of the MT secretion fluid, with simultaneous maintenance of hemolymph $[Na^+]$ and $[K^+]$ suggests that the MTs may help conserve hemolymph Na^+ and K^+ by suppressing Na^+ and K^+ transport to potentially overcome an imbalance of these ions at the whole-animal level resulting from the cumulative effect of diminished AaAQP5 in the various osmoregulatory organs. The distal MT secretion fluid is normally iso-osmotic to the hemolymph, and assuming this remained consistent in the AaAQP5 knockdown

MTs, the changes in cationic concentrations observed in this study suggest osmotic compensation from other osmolytes, perhaps proline and trehalose, via alternative pathways (Akhter et al., 2017; Beyenbach, 2003; Yerushalmi et al., 2016). These altered ion concentrations may be a result of overall metabolic suppression or a decrease in the molecular capacity for ATP synthesis. Alternatively, the changes in the ion transport rate may be a consequence of individual transporter regulation (Esquivel et al., 2016). The localization of AaAQP5 and the site of Na^+/K^+ transport coincide in the principal cells. A knockdown of AaAQP5 in the principal cells would therefore have direct effects on principal cell function, which could lead to a compensatory regulation of individual transporters. The transepithelial Cl^- pathway in adult *A. aegypti* MTs transpires through the paracellular pathway as well as through stellate cells, although both theories have been debated in the past (Beyenbach, 2003; Beyenbach and Piermarini, 2011; O'Connor and Beyenbach, 2001; O'Donnell et al., 1996; Yu and Beyenbach, 2001). The maintenance of high transepithelial Cl^- transport rates suggests a lack of Cl^- transport regulation in the MTs in response to AaAQP5 knockdown. Furthermore, as Cl^- typically serves to balance the electrical charge from cation transport, this result suggests that other positively charged solutes such as NH_4^+ may be transported in greater amounts by the AaAQP5 knockdown MTs. Interestingly, the unaltered Cl^- secretion rate coupled with a decrease in overall fluid secretion is expected to result in a decrease in hemolymph $[\text{Cl}^-]$, which was supported by our findings.

AQP5 knockdown affects survival

AQP5 knockdown decreased the survival of larval *A. aegypti*, throughout a 6 day period following dsRNA exposure (Fig. 4). We demonstrated that MT function is altered with AaAQP5 knockdown such that MTs exhibit reduced rates of fluid, Na^+ and K^+ transport; however, this did not affect total body moisture (Fig. 5) or hemolymph $[\text{Na}^+]$ and $[\text{K}^+]$ (Fig. 6). Knockdown of AaAQP5 in adult *A. aegypti* enhanced survival by 1–2 h in a desiccating environment (Drake et al., 2015). In contrast, knockdown of AgAQP1 and AgAQP3 in *A. gambiae* using dsRNA exhibited reduced survival of adult females compared with controls under arid environmental conditions (Liu et al., 2011, 2016). These differences in the effects of AQP knockdown on survival are likely to reflect organ-specific expression of these individual AQPs and the functional role of these organs in the physiology of the insect would undoubtedly impinge on survival in response to AQP knockdown. For example, AaAQP5 in the anal papillae of *A. aegypti* larvae is likely to contribute to osmoregulation as AaAQP5 expression is dependent on external salinity such that it is abundantly expressed in high-salinity environments (Akhter et al., 2017). In this respect, we would not expect the knockdown of AaAQP5 in anal papillae to have contributed to the observations made in this study because AaAQP5 levels are relatively low in the anal papillae of freshwater-reared larvae. However, it is expected that AaAQP5 knockdowns in high-salinity environments will have a significant impact on larval survival. Aqp7777 (RE34617) of *D. melanogaster* demonstrated high expression in the brain and segmental ganglia as well as the body wall and visceral muscles, which may all contribute to the overall survival of the animal (Kaufmann et al., 2005). Therefore, decreased survival of the larvae with reduced AaAQP5 expression may have resulted from organs not responsible for osmo- and ion regulation. Future work should therefore assess the expression of AaAQP5 in the other osmoregulatory organs and the effects of dsRNA treatment on these organs.

Conclusion

Our previous studies detected relatively high transcript abundance of AaAQP1, AaAQP4 and AaAQP5 in larval *A. aegypti* MTs (Marusalin et al., 2012). In this study, we demonstrated that AaAQP5 protein is expressed by principal cells where it is localized on both the basal and the apical membranes. Knockdown of AaAQP5 significantly decreased fluid secretion rates of MTs. Together, the results implicate AaAQP5 in mediating water transport by the MTs of larval *A. aegypti*. The alterations in $[\text{Na}^+]$ and $[\text{K}^+]$ of the secreted fluid were unexpected and may indicate that MTs can adjust ion transport in response to impaired fluid transport. As larvae inhabit freshwater, the production of a dilute urine, which conserves ions while eliminating excess water is crucial to survival and this process begins with fluid secretion by the MTs. Our results indicate that AaAQP5 plays an important role in this vital process.

Acknowledgements

The authors thank Helen Chasiotis for technical training and primer design.

Competing interests

The authors declare no competing or financial interests.

Author contributions

Conceptualization: L.M., A.D.; Methodology: L.M., G.Y.Y., A.D.; Validation: L.M., G.Y.Y.; Formal analysis: L.M.; Investigation: L.M., G.Y.Y.; Resources: A.D.; Data curation: L.M.; Writing - original draft: L.M.; Writing - review & editing: L.M., G.Y.Y., A.D.; Visualization: L.M.; Supervision: A.D.; Project administration: L.M., A.D.; Funding acquisition: A.D.

Funding

This study was funded by the Natural Sciences and Engineering Research Council of Canada (grant 355910-2013).

References

- Aitken, T. H. G., Tesh, R. B., Beaty, B. J. and Rosen, L. (1979). Transovarial transmission of yellow fever virus by mosquitoes (*Aedes aegypti*). *Am. J. Trop. Med. Hyg.* **28**, 119–121.
- Akhter, H., Misyura, L., Bui, P. and Donini, A. (2017). Salinity responsive aquaporins in the anal papillae of the larval mosquito, *Aedes aegypti*. *Comp. Biochem. Physiol. A Mol. Integr. Physiol.* **203**, 144–151.
- Benoit, J. B., Hansen, I. A., Attardo, G. M., Michalková, V., Mireji, P. O., Bargul, J. L., Drake, L. L., Masiga, D. K. and Aksoy, S. (2014). Aquaporins are critical for provision of water during lactation and intrauterine progeny hydration to maintain tsetse fly reproductive success. *PLoS Negl. Trop. Dis.* **8**, e2517.
- Beyenbach, K. W. (2003). Transport mechanisms of diuresis in Malpighian tubules of insects. *J. Exp. Biol.* **206**, 3845–3856.
- Beyenbach, K. W. and Piermarini, P. M. (2011). Transcellular and paracellular pathways of transepithelial fluid secretion in Malpighian (renal) tubules of the yellow fever mosquito *Aedes aegypti*. *Acta Physiol.* **202**, 387–407.
- Bhatt, S., Gething, P. W., Brady, O. J., Messina, J. P., Farlow, A. W., Moyes, C. L., Drake, J. M., Brownstein, J. S., Hoen, A. G., Sankoh, O. et al. (2013). The global distribution and burden of dengue. *Nature* **496**, 504–507.
- Bradley, T. J. (1987). Physiology of osmoregulation in mosquitoes. *Annu. Rev. Entomol.* **32**, 439–462.
- Bradley, T. J., Snyder, C. (1989). Fluid secretion and microvillar ultrastructure in mosquito Malpighian tubules. *Am. J. Physiol.* **257**, R1096–R1102.
- Campbell, E. M., Ball, A., Hoppler, S. and Bowman, A. S. (2008). Invertebrate aquaporins: a review. *J. Comp. Physiol. B* **178**, 935–955.
- Chasiotis, H., Ionescu, A., Misyura, L., Bui, P., Fazio, K., Wang, J., Patrick, M., Weihrauch, D. and Donini, A. (2016). An animal homolog of plant Mep/Amt transporters promotes ammonia excretion by the anal papillae of the disease vector mosquito, *Aedes aegypti*. *J. Exp. Biol.* **219**, 1346–1355.
- Clark, T. M. and Bradley, T. J. (1996). Stimulation of Malpighian tubules from larval *Aedes aegypti* by secretagogues. *J. Insect Physiol.* **42**, 593–602.
- Cymer, F. and Schneider, D. (2010). A single glutamate residue controls the oligomerization, function, and stability of the aquaglyceroporin GlpF. *Biochemistry* **49**, 279–286.
- Donini, A. and O'Donnell, M. (2005). Analysis of Na^+ , Cl^- , K^+ , H^+ and NH_4^+ concentration gradients adjacent to the surface of anal papillae of the mosquito *Aedes aegypti*: application of self-referencing ion-selective microelectrodes. *J. Exp. Biol.* **208**, 603–610.
- Donini, A., Patrick, M. L., Bijelic, G., Christensen, R. J., Janowski, J. P., Rheault, M. R. and O'Donnell, M. J. (2006). Secretion of water and ions by malpighian

- tubules of larval mosquitoes: effects of diuretic factors, second messengers, and salinity. *Physiol. Biochem. Zool.* **79**, 645-655.
- Drake, L. L., Boudko, D. Y., Marinotti, O., Carpenter, V. K., Dawe, A. L. and Hansen, I. A.** (2010). The Aquaporin gene family of the yellow fever mosquito, *Aedes aegypti*. *PLoS ONE* **5**, e15578.
- Drake, L. L., Rodriguez, S. D. and Hansen, I. A.** (2015). Functional characterization of aquaporins and aquaglyceroporins of the yellow fever mosquito, *Aedes aegypti*. *Sci. Rep.* **5**, 7795.
- Echevarría, M., Ramírez-Lorca, R., Hernández, C. S., Gutiérrez, A., Méndez-Ferrer, S., González, E., Toledo-Aral, J. J., Ilundáin, A. A. and Whittombury, G.** (2001). Identification of a new water channel (Rp-MIP) in the Malpighian tubules of the insect *Rhodnius prolixus*. *Pflügers Arch. Eur. J. Physiol.* **442**, 27-34.
- Esquivel, C. J., Cassone, B. J. and Piermarini, P. M.** (2016). A de novo transcriptome of the Malpighian tubules in non-blood-fed and blood-fed Asian tiger mosquitoes *Aedes albopictus*: insights into diuresis, detoxification, and blood meal processing. *PeerJ* **4**, e1784.
- Finn, R. N., Chauvigné, F., Stavang, J. A., Belles, X. and Cerdà, J.** (2015). Insect glycerol transporters evolved by functional co-option and gene replacement. *Nat. Commun.* **6**, 7814.
- García, F., Kierbel, A., Larocca, M. C., Gradihone, S. A., Splinter, P., LaRusso, N. F. and Marinelli, R. A.** (2001). The water channel aquaporin-8 is mainly intracellular in rat hepatocytes, and its plasma membrane insertion is stimulated by cyclic AMP. *J. Biol. Chem.* **276**, 12147-12152.
- Gonzales, K. K., Tsujimoto, H. and Hansen, I. A.** (2015). Blood serum and BSA, but neither red blood cells nor hemoglobin can support vitellogenesis and egg production in the dengue vector *Aedes aegypti*. *PeerJ* **3**, e938.
- Hegarty, J. L., Zhang, B., Carroll, M. C., Cragoe, E. J. and Beyenbach, K. W.** (1992). Effects of amiloride on isolated Malpighian tubules of the yellow fever mosquito (*Aedes aegypti*). *J. Insect Physiol.* **38**, 329-337.
- Hendriks, G., Koudijs, M., van Balkom, B. W. M., Oorschot, V., Klumperman, J., Deen, P. M. T. and van der Sluijs, P.** (2004). Glycosylation is important for cell surface expression of the water channel aquaporin-2 but is not essential for tetramerization in the endoplasmic reticulum. *J. Biol. Chem.* **279**, 2975-2983.
- Jonusaite, S., Kelly, S. P. and Donini, A.** (2011). The physiological response of larval *Chironomus riparius* (Meigen) to abrupt brackish water exposure. *J. Comp. Physiol. B* **181**, 343-352.
- Kambara, K., Takematsu, Y., Azuma, M. and Kobayashi, J.** (2009). cDNA cloning of aquaporin gene expressed in the digestive tract of the Formosan subterranean termite, *Coptotermes formosanus* Shiraki (Isoptera; Rhinotermitidae). *Appl. Entomol. Zool.* **44**, 315-321.
- Kaufmann, N., Mathai, J. C., Hill, W. G., Dow, J. A. T., Zeidel, M. L. and Brodsky, J. L.** (2005). Developmental expression and biophysical characterization of a *Drosophila melanogaster* aquaporin. *Am. J. Physiol. Cell Physiol.* **289**, C397-C407.
- Kobayashi, H., Yokoo, H., Yanagita, T., Satoh, S., Kis, B., Deli, M., Niwa, M. and Wada, A.** (2006). Induction of aquaporin 1 by dexamethasone in lipid rafts in immortalized brain microvascular endothelial cells. *Brain Res.* **1123**, 12-19.
- Kraemer, M. U. G., Sinka, M. E., Duda, K. A., Mylne, A., Shearer, F. M., Barker, C. M., Moore, C. G., Carvalho, R. G., Coelho, G. E., Van Bortel, W. et al.** (2015). The global distribution of the arbovirus vectors *Aedes aegypti* and *Ae. albopictus*. *Elife* **4**, e08347.
- Liu, K., Tsujimoto, H., Cha, S.-J., Agre, P. and Rasgon, J. L.** (2011). Aquaporin water channel AgAQP1 in the malaria vector mosquito *Anopheles gambiae* during blood feeding and humidity adaptation. *Proc. Natl. Acad. Sci. USA* **108**, 6062-6066.
- Liu, K., Tsujimoto, H., Huang, Y., Rasgon, J. L. and Agre, P.** (2016). Aquaglyceroporin function in the malaria mosquito *Anopheles gambiae*. *Biol. Cell* **108**, 294-305.
- Martini, S. V., Goldenberg, R. C., Fortes, F. S. A., Campos-de-Carvalho, A. C., Falkenstein, D. and Morales, M. M.** (2004). *Rhodnius prolixus* Malpighian tubule's aquaporin expression is modulated by 5-hydroxytryptamine. *Arch. Insect Biochem. Physiol.* **57**, 133-141.
- Marusalin, J., Matier, B. J., Rheault, M. R. and Donini, A.** (2012). Aquaporin homologs and water transport in the anal papillae of the larval mosquito, *Aedes aegypti*. *J. Comp. Physiol. B* **182**, 1047-1056.
- Neely, J. D., Christensen, B. M., Nielsen, S. and Agre, P.** (1999). Heterotetrameric composition of aquaporin-4 water channels. *Biochemistry* **38**, 11156-11163.
- O'Connor, K. and Beyenbach, K.** (2001). Chloride channels in apical membrane patches of stellate cells of Malpighian tubules of *Aedes aegypti*. *J. Exp. Biol.* **204**, 367-378.
- O'Donnell, M. J., Dow, J. A., Huesmann, G. R., Tublitz, N. J. and Maddrell, S. H.** (1996). Separate control of anion and cation transport in Malpighian tubules of *Drosophila melanogaster*. *J. Exp. Biol.* **199**, 1163-1175.
- Overend, G., Cabrero, P., Halberg, K. A., Ranford-Cartwright, L. C., Woods, D. J., Davies, S. A. and Dow, J. A. T.** (2015). A comprehensive transcriptomic view of renal function in the malaria vector, *Anopheles gambiae*. *Insect Biochem. Mol. Biol.* **67**, 47-58.
- Petzel, D. H., Pirotte, P. T. and Van Kerkhove, E.** (1999). Intracellular and luminal pH measurements of Malpighian tubules of the mosquito *Aedes aegypti*: the effects of cAMP. *J. Insect Physiol.* **45**, 973-982.
- Pietrantonio, P. V., Jagge, C., Keeley, L. L. and Ross, L. S.** (2000). Cloning of an aquaporin-like cDNA and in situ hybridization in adults of the mosquito *Aedes aegypti* (Diptera: Culicidae). *Insect Mol. Biol.* **9**, 407-418.
- Preston, G. M., Jung, J. S., Guggino, W. B. and Agre, P.** (1993). The mercury-sensitive residue at cysteine 189 in the CHIP28 water channel. *J. Biol. Chem.* **268**, 17-20.
- Rueda, L. M.** (2008). Global diversity of mosquitoes (Insecta: Diptera: Culicidae) in freshwater. *Hydrobiologia* **595**, 477-487.
- Schneider, C. A., Rasband, W. S. and Eliceiri, K. W.** (2012). NIH Image to ImageJ: 25 years of image analysis. *Nat. Methods* **9**, 671-675.
- Smith, B. and Agre, P.** (1991). Erythrocyte Mr 28,000 transmembrane protein exists as a multisubunit oligomer similar to channel proteins. *J. Biol. Chem.* **266**, 6407-6415.
- Smith, P. J. S., Hammar, K., Porterfield, D. M., Sanger, R. H. and Trimarchi, J. R.** (1999). Self-referencing, non-invasive, ion selective electrode for single cell detection of trans-plasma membrane calcium flux. *Microsc. Res. Tech.* **46**, 398-417.
- Stobart, R.** (1971). Factors affecting the control of body volume in the larvae of the mosquitoes *Aedes aegypti* (L.) and *Aedes detritus*. *J. Exp. Biol.* **54**, 67-82.
- Tomkowiak, E. and Pienkowska, J. R.** (2010). The current knowledge of invertebrate aquaporin water channels with particular emphasis on insect AQP. *Adv. Cell Biol.* **2**, 91-104.
- Tsujimoto, H., Liu, K., Linser, P. J., Agre, P. and Rasgon, J. L.** (2013). Organ-specific splice variants of aquaporin water channel AgAQP1 in the malaria vector *Anopheles gambiae*. *PLoS ONE* **8**, e75888.
- Van Ekert, E., Chauvigné, F., Finn, R. N., Mathew, L. G., Hull, J. J., Cerdà, J. and Fabrick, J. A.** (2016). Molecular and functional characterization of *Bemisia tabaci* aquaporins reveals the water channel diversity of hemipteran insects. *Insect Biochem. Mol. Biol.* **77**, 39-51.
- Weng, X.-H., Huss, M., Wiczorek, H. and Beyenbach, K. W.** (2003). The V-type H⁺-ATPase in Malpighian tubules of *Aedes aegypti*: localization and activity. *J. Exp. Biol.* **206**, 2211-2219.
- Wigglesworth, V. B.** (1932). The function of the anal gills of the mosquito larva. *J. Exp. Biol.* **10**, 16-26.
- Williams, J. C. and Beyenbach, K. W.** (1983). Differential effects of secretagogues on Na and K secretion in the Malpighian tubules of *Aedes aegypti* (L.). *J. Comp. Physiol.* **149**, 511-517.
- Wright, P. A.** (1995). Nitrogen excretion: three end products, many physiological roles. *J. Exp. Biol.* **198**, 273-281.
- Yerushalmi, G. Y., Misyura, L., Donini, A. and MacMillan, H. A.** (2016). Chronic dietary salt stress mitigates hyperkalemia and facilitates chill coma recovery in *Drosophila melanogaster*. *J. Insect Physiol.* **95**, 89-97.
- Yu, M.-J. and Beyenbach, K. W.** (2001). Leucokinin and the modulation of the shunt pathway in Malpighian tubules. *J. Insect Physiol.* **47**, 263-276.